



HAL
open science

Orange hydrogen is the new green

Florian Osselin, Cyprien Soulaine, C. Fauguerolles, E. C. Gaucher, Bruno Scaillet, Michel Pichavant

► **To cite this version:**

Florian Osselin, Cyprien Soulaine, C. Fauguerolles, E. C. Gaucher, Bruno Scaillet, et al.. Orange hydrogen is the new green. *Nature Geoscience*, 2022, 15, pp.765-769. 10.1038/s41561-022-01043-9 . insu-03858117

HAL Id: insu-03858117

<https://insu.hal.science/insu-03858117v1>

Submitted on 18 Nov 2022

HAL is a multi-disciplinary open access archive for the deposit and dissemination of scientific research documents, whether they are published or not. The documents may come from teaching and research institutions in France or abroad, or from public or private research centers.

L'archive ouverte pluridisciplinaire **HAL**, est destinée au dépôt et à la diffusion de documents scientifiques de niveau recherche, publiés ou non, émanant des établissements d'enseignement et de recherche français ou étrangers, des laboratoires publics ou privés.

Orange hydrogen is the new Green

F. Osselin^{1*}, C. Soullaine¹, C. Fauguerolles¹, E. C. Gaucher², B. Scaillet¹ and M. Pichavant¹

^{1*}Institut des Sciences de la Terre d'Orléans, Université d'Orléans, CNRS, BRGM UMR7327, 1A Rue de la Ferrollerie, 45100 Orléans, France.

²Institute of Geological Science, Bern University..

1 Abstract

Maintaining the global warming well below 2°C, as stipulated in the Paris Agreement, will require a complete overhaul of the world energy system. Hydrogen is considered to be a key component of the decarbonization strategy for large parts of the transport system, as well as some heavy industries. Today, about 96% of current hydrogen production comes from the steam reforming of coal or natural gas (labeled Black and Grey hydrogen, respectively). If hydrogen is to become a solution, then Black and Grey hydrogen need to be replaced by a low-carbon option. One method that has received much attention is to produce so-called Green hydrogen by coupling water electrolysis with renewable energies. However, green hydrogen is expensive and energy intensive to produce. In this communication, we explore an alternative option and highlight the benefits of rock-based hydrogen (White and Orange) compared with classic electrolysis-based technologies. We show that the exploitation of native

001
002
003
004
005
006
007
008
009
010
011
012
013
014
015
016
017
018
019
020
021
022
023
024
025
026
027
028
029
030
031
032
033
034
035
036
037
038
039
040
041
042
043
044
045
046

047 hydrogen and its combination with carbon sequestration has the potential to
048 fuel a large part of the energy transition without the substantial energy and
049 raw material cost of Green hydrogen.
050
051

052

053

054 **2 Main**

055

056 To meet the Net Zero Emission Scenario (NZE) of the International Energy
057 Agency [1], about 17,000 TWh of hydrogen-based energy will be consumed
058 in the world in 2050. This hydrogen is usually seen as being provided by
059 large facilities using renewable electricity to convert water to hydrogen through
060 electrolysis (Green hydrogen). The energy cost for hydrogen production is
061 related to the splitting of the water molecule into hydrogen and oxygen:
062
063
064
065
066

067



069

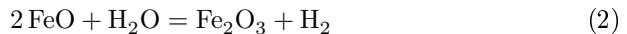
070 and is directly calculated from the Gibbs energy of formation of water (120
071 MJ/kg_{H₂} at 25°C – THERMODDEM database [2]). Considering an 80% effi-
072 cient electrolyser, this corresponds to about 400 Mt of hydrogen, or about five
073 times the amount consumed in 2020 [1]. These 17,000 TWh represent more
074 than the electricity produced by both China and the USA in 2020, about 63%
075 of the world’s electricity production, and more than twice the current world-
076 wide production of electricity from renewable energies. Meeting this figure will
077 then require an unprecedented upscaling of both electrolysis and renewable
078 energies.
079
080
081
082
083
084

085 Blue hydrogen does not fare better due to the extra cost related to CCS
086 and is probably only a temporary solution [3]. Some authors are even more
087 critical, arguing that the imperfect capture of CO₂ associated with methane
088 losses along the whole chain leads to increased greenhouse gas emissions with
089 only little benefits from pure Grey hydrogen [4]. Another critical shortcoming
090
091
092

of Blue hydrogen is the continued reliance on fossil fuel. This last issue also impacts an emerging production technique, sometimes referred to as Turquoise, and which consists in producing H₂ from methane but with graphite-C and not CO₂ as a resulting product. This technology is still in development but could also play a key role in the coming years.

3 A greener hydrogen

The Earth's subsurface is a giant and undervalued hydrogen factory. Long considered anecdotic, the current estimations give a rough estimate of 20 Mt of native hydrogen escaping from the surface towards the atmosphere each year [5]. Estimates vary widely but everything suggests that the subsurface is actually producing significantly more, and that this value is just the tip of the iceberg. Natural hydrogen is most commonly produced by the reduction of water to hydrogen following the anoxic and abiotic oxidation of ferrous iron to the orange-coloured ferric iron [6]:



This oxidation occurs, for example, under the ocean floor [7, 8], where peridotites – magnesium silicate rocks which contain up to 10%wt of ferrous iron – become hydrated at temperatures between 200 and 400°C by the percolation of seawater. This process, known as serpentinization, also occurs at lower temperatures and pressures on land-based ophiolite-peridotite massifs [9]. Serpentinization is estimated to produce around 1-2 Mt of hydrogen per year [10] at oceanic ridges where it is the most active. However, serpentinization is not the only process producing hydrogen and anywhere water meets reduced iron, there is a possibility to produce hydrogen if the right conditions of temperature, fluid composition and pressure are met (e.g. archaean

4 *Orange hydrogen is the new Green*

139 Banded-Iron Formations [11], peralkaline and biotite-rich granites [12, 13]).
140 On land, numerous native hydrogen seeps (usually mixed with methane [14])
141 have been localized (e.g. Oman, Japan, New Caledonia, Greece, Spain, Italy,
142 California) [15], France [16], Australia, Brazil [17], Kansas [18]). Some are even
143 known since the antiquity such as the Mount Chimaera (Yanartaş, Turkey)
144 which continuously produces a mixture of 87%*vol.* CH₄ and 10%*vol.* H₂ [14].
145 Exploitation of this hydrogen offers then an interesting alternative to Green
146 and Blue hydrogen by completely skipping the electrolysis and simply col-
147 lecting the hydrogen emitted by natural underground processes. This White
148 hydrogen is already under production in Mali where a well drilled for water
149 turned out to produce a 98%*vol* hydrogen stream currently used power the
150 entire village of Bourakebougou for the last 10 years [19]. The actual source
151 of the hydrogen remains unknown but chances are that the reduction of iron
152 is involved deep underground.
153
154
155
156
157
158
159
160
161
162
163

164 4 Orange Hydrogen

165 It is possible to go even further and go Orange. This color, which refers to
166 the color of oxidized iron, follows the same principles of White hydrogen and
167 looks to make the Earth provide most of the work for hydrogen production.
168 Yet, instead of using a passive approach of exploration/exploitation, Orange
169 hydrogen follows a proactive way and searches to stimulate the reaction. This
170 is done by injecting water *in situ* in identified reactive formations and collect
171 the hydrogen-saturated water from recovery wells surrounding the injection
172 point (Fig. 1). This approach can also be adopted for Fe-rich mine wastes and
173 steel slags [20] in an *ex situ* surface reactor which has the advantage of being
174 easier to control and set-up. Additionally, the magnetite particles (Fe₃O₄)
175 resulting from the oxidation process have a commercial value, especially in
176
177
178
179
180
181
182
183
184

the pharmaceutical industry. However, the significantly lower volumes of raw materials available for *ex situ* Orange Hydrogen and the prohibitive financial and environmental cost of extracting and grinding new feedstock makes the *ex situ* solution less attractive than the *in situ* one.

In situ Orange hydrogen requires more energy than White hydrogen production, but the outputs will be significantly higher, while production costs will likely remain under Blue/Green ones. An average peridotite can provide around 2-4 kg_{H₂}/m³ upon complete oxidation. With 10²⁰ kg of peridotites in the upper crust (top 7km) [21], there are 100 trillions tons of hydrogen to be extracted from the subsurface, sufficient for 250,000 years at a rate of 400 Mt/year. This is not even considering that over these timescales, tectonic activity will refresh the peridotites at a rate of 10¹² kg/year [21]. The exploitation of the whole volume is obviously unrealistic due to technical, economic and regulatory reasons, but even a small percentage would make Orange hydrogen a key player in the achievement of the NZE scenario.

The real game-changing impact of Orange hydrogen, is that the very same formations which naturally produce hydrogen are also the perfect location for carbon sequestration [22]. These formations are part of the deep carbon cycle, balancing the concentration of atmospheric carbon dioxide through its reaction with silicate rocks. This natural weathering has allowed the capture of 99.9% of the total carbon on Earth as solid, stable carbonates [23], but is now getting rapidly outpaced by the increase in anthropic emissions since the industrial era. Matter *et al.* [24] calculated for example that 30 trillions tons of CO₂ can be stored in the Oman Ophiolite (the largest on-land peridotite massif), and 100 trillions tons globally. For comparison, the CO₂ anthropic emissions in 2020 are estimated at 33 billions tons.

185
186
187
188
189
190
191
192
193
194
195
196
197
198
199
200
201
202
203
204
205
206
207
208
209
210
211
212
213
214
215
216
217
218
219
220
221
222
223
224
225
226
227
228
229
230

231 In Iceland, Carbfix, a company built on the results of several European
232 Union's research projects, has been injecting 72,000 tons of carbon dioxide
233 in the island basaltic formation for about 10 years with great success [25,
234 235 26]. A similar pilot injected 1000 tons of pure liquid CO₂ in the Columbia
236 River Basalts near Wallula (USA). Cores retrieved 2 years after the injection
237 presented unequivocal evidence of the mineralization of the injected CO₂ [27].
238 However, neither of these large-scale pilots considered the hydrogen production
239 associated with the CO₂ mineralization process despite the iron-rich nature of
240 the targeted basalts and thus the possibility of coupled production [28].
241

242 The list of Orange hydrogen advantages does not end here. In contrast to
243 electrolysis, where only specifically tuned water compositions can be used, nat-
244 245 246 247 248 249 250 251 252 253 254 255 256 257 258 259 260 261 262 263 264 265 266 267 268 269 270 271 272 273 274 275 276
269 ural oxidation of iron as well as carbon mineralization works very well with
270 seawater [29] or even wastewater, alleviating significantly the water cost of
271 hydrogen production. Target formations can also contain elements of economic
272 interest such as Li, Ni, Co... as is usually the case in serpentinite formations
273 [30]. The dissolution of the primary minerals following the injection will release
274 these elements in the percolating fluids, which can be extracted in parallel to
275 hydrogen by fractionated precipitation. Similar processes are currently in use
276 in Uranium recovery [31] and extraction of Li in parallel to heat is being con-
sidered in geothermal applications [32]. Orange hydrogen differs significantly
from the alternatives as it does not rely on critical raw materials as electrolysis
processes, and can even produce them as by-products of the main operation.

269 Laboratory experiments on the reactivity of magnesium silicates with car-
270 271 272 273 274 275 276
270 bon dioxide have shown that a mixture of NaHCO₃ and dissolved CO₂ can
271 achieve complete carbonation over the course of a few hours to a few days [33].
272 Carbonation rate is a direct function of the CO₂ partial pressure but the rate
273 of serpentinization seems either unaffected [34] or slightly accelerated [35] by

the presence of CO₂. Both carbonation and serpentinization reaction rates are also strongly temperature-dependent, and follow a bell-shaped curve with an maximum respectively at 185°C and between 250 and 280°C for serpentinization [36, 37]. Maintaining a high rate of H₂ production and CO₂ mineralization requires thus a careful control of the downhole temperature. Luckily, serpentinization and carbonation are very exothermic (respectively $\Delta H = 250$ kJ/kg and $\Delta H = 760$ kJ/kg). Once the process is initiated, the desired temperature can be obtained through self-heating with a heat production from the chemical reactions balancing the heat losses through convection and conduction, as well as the cooling induced by the injection of colder fluids [24, 38]. This self-heating behavior allows reducing production costs as no surface heating of the injected fluids is necessary, but requires a careful control of the injection rate. Interestingly, some of this heat can be extracted from the recovered fluids in a geothermal-like process and be reused to power the facility with recovered fluid temperatures up to 200-300°C (considering the combined action of exothermic reaction and formation temperatures e.g. 250°C for Carbfix2 [39]).

Kelemen *et al.* [38] calculate a carbonation rate of 4.10^9 tCO₂/year for the stimulation of 1 km³ of peridotite at 185°C (5.10^6 kg/s of carbonation, CO₂ partial pressure between 75 and 300 bars). Extrapolating their calculation with 10%wt FeO, this leads to a rate of 5 Mt_{H₂}/year for 1 km³ of peridotite (5.10^4 kg/s for serpentinization in the same conditions). In Figure 2 are represented hydrogen production rates from batch [40–42] and reactive percolation [43] experiments. In all cases, measured hydrogen production is significant and approaches the maximum production which can be expected from these rocks. A linear fit of the data gives rates from 0.1 to 3 Mt_{H₂}/km³/year, similar to the extrapolation from Kelemen *et al.* [38]. As a result, experimental

277
278
279
280
281
282
283
284
285
286
287
288
289
290
291
292
293
294
295
296
297
298
299
300
301
302
303
304
305
306
307
308
309
310
311
312
313
314
315
316
317
318
319
320
321
322

323 data from laboratory experiments support directly the preliminary estima-
324 tions. Extra research is however necessary to assess the potential of other types
325 of formations for hydrogen production combined with carbon sequestration.
326

327 This means that, while it is not expected that Orange hydrogen will solely
328 meet the 400 Mt for the NZE scenario, it has the potential to provide a sig-
329 nificant part of it, at a fraction of the energy and raw/critical mineral cost of
330 electrolyzers. In other words, Orange hydrogen promises to provide abundant,
331 clean, rock-based, carbon-negative, and price-competitive energy to fuel the
332 energy transition towards the NZE scenario.
333
334
335
336
337
338
339
340

341 5 Challenges for Orange hydrogen

342
343 Developing Orange hydrogen faces numerous scientific challenges, which can
344 be sorted in 3 different categories:
345

- 346
347 1. Accurate description, quantification and mapping of the resource, taking
348 into account the iron grade of the targeted rock formation and its technical
349 and societal accessibility.
350
351
352
- 353 2. Identification of the ideal pressure, temperature, flow rate, fluid composi-
354 tion for the optimized production of hydrogen and carbon mineralization.
355
356 These settings need to account for the precipitation of parasitic minerals
357 competing with carbonate precipitation, the incorporation of Fe into pre-
358 cipitating minerals preventing its oxidation and H₂ production, as well as
359 the careful control of porosity to prevent any clogging by the precipitat-
360 ing minerals. Parasitic reactions are for example at work in the experiment
361 from Grozeva *et al.* [41] represented on Figure 2. The injection of a CO₂-rich
362 fluid mid-experiment lead to a decrease in H₂ in the reactor. The process
363 consuming the hydrogen was however, not clearly identified.
364
365
366
367
368

3. Field-scale optimization of the injection and recovery of the fluids to maximize the impacted zone and minimize hydrogen losses. This includes research on reservoir stimulation (hydraulic fracturing and chemical stimulation) and potential induced (micro)-seismicity, as well as the microbiology of low-temperature reservoirs which, if left unchecked, can consume the produced H₂ and impact significantly the yield.

These challenges cover a wide range of scales and disciplines and require a combined effort to offer a satisfactory solution. The first challenge falls within the scope of geologists and economists, the second is related to thermodynamics and geochemistry as well as the physics of coupled processes in porous media. The third one concerns reservoir engineering and simulations, geotechnics and microbiology. Given the scale of the projects, social acceptance will also be a key point in the development of the technology, in particular in the case of induced-seismicity.

One example of these multidisciplinary and multiscale challenges is the proper modeling of the porosity/permeability relationship during the process. Carbonation of target rocks leads to the precipitation of carbonate minerals within the porosity as well as the precipitation of serpentine, which is less dense than the minerals it replaces. As such, the porosity and thus the permeability of the rock will be a function of the dynamic balance between dissolution of the primary minerals and the precipitation of the secondary minerals. If the latter occurs faster, it is likely that some clogging will occur with dramatic effects on the long-term viability of the process. Yet, the only two large-scale pilots for geological mineralization of CO₂ have not evidenced any clogging or permeability decrease, even several years after the beginning of the injection in the case of Carbfix [26]. Moreover, natural settings are proofs that carbonation can be going on for tens to hundreds of thousands of years without any clogging [44].

415 Reaction-induced fracturing, which is often invoked to explain the maintained
416 permeability during some natural processes despite adverse molar volume evo-
417 lution is the process during which a growing mineral in a confined space is able
418 to generate large stresses on the surrounding matrix, enough to fracture it and
419 open new percolation paths for the fluid [45–47]. However, up to date, not only
420 does the modeling of such fracturing still fail to reproduce the experimental
421 observations but experiments of reactive percolation where such phenomenon
422 is expected, usually do not present any evidence that reactive-induced fractur-
423 ing occurred [43, 48, 49]. The control of reaction-induced fracturing and the
424 overall control of the reactivity and injectivity during the production of Orange
425 hydrogen (potentially through targeted hydraulic fracturing) is of paramount
426 importance for the viability of the process and requires a deeper understand-
427 ing of the microscopic behavior of dissolution/precipitation as well as a proper
428 upscaling of these processes to reservoir and field scale.
429
430
431
432
433
434
435
436
437
438
439
440
441
442
443

444 **6 Conclusion**

445
446 We are at a tipping point for the climate, and the exploitation of Orange
447 hydrogen is an additional technology which could prevent a dramatic evolu-
448 tion. Hydrogen is nowadays a controversial energy carrier as it is considered
449 by some as an easy way to transport energy and decarbonize the transporta-
450 tion sector, while others see it as an unnecessary intermediate and advocate a
451 full electric switch. This controversy becomes irrelevant if White and Orange
452 hydrogen are included in the debate. Their production does not require as
453 much electricity or raw materials as Green hydrogen and Orange hydrogen
454 offers also the possibility to store enough CO₂ to curb global warming.
455
456
457
458
459
460

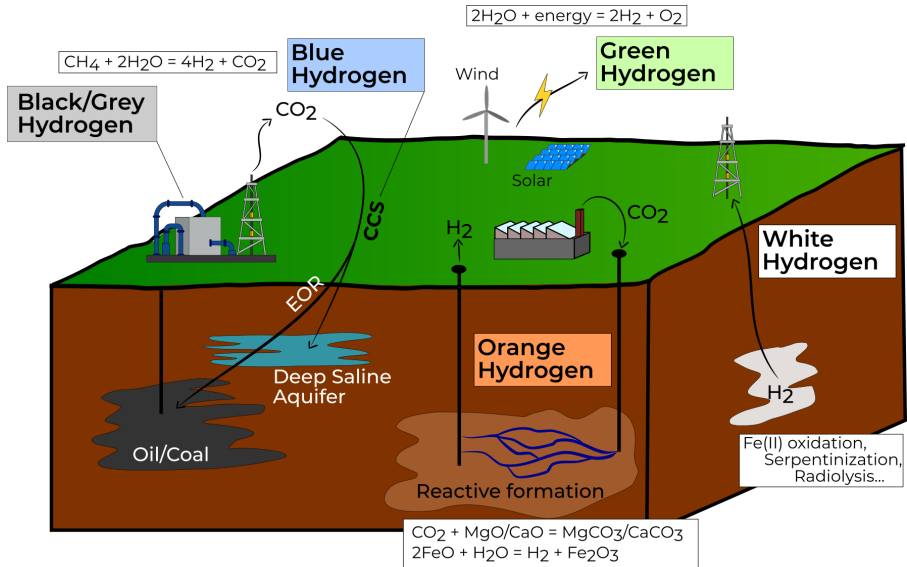
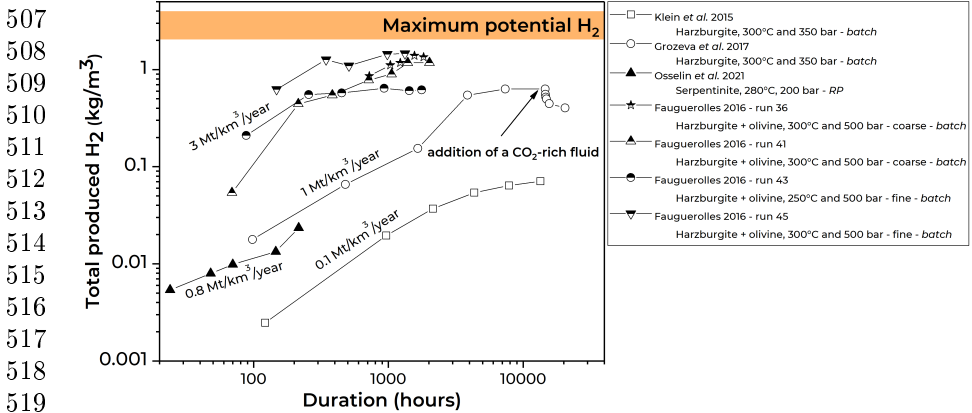


Fig. 1 The different colors of Hydrogen. Black/Grey H₂ is from steam reforming. It turns Blue through the addition of CCS, either through permanent storage (e.g. in deep saline aquifers) or through Enhanced Oil Recovery (EOR). On the other end of the spectrum, Green hydrogen is produced by electrolysis using renewable energies. White hydrogen corresponds to the exploitation of subsurface-sourced natural hydrogen. Orange hydrogen is a proactive take on White hydrogen and consists in injecting in a reactive formation a carbon-enriched solution. Geochemical reactions lead to the precipitation of solid carbonates while hydrogen is formed and recovered from the fluid.

In addition to energy considerations, the decarbonization of the world's energy mix will require an unprecedented upscaling in the production of renewable energies and the associated batteries and thus in ore mining, especially for Nickel-Cobalt ($\times 20 - 25$) and Lithium ($\times 40$) [50]. Every million tons of White and Orange hydrogen means at least 120 TJ (or 33GWh) of electricity saved. This saved electricity as well as the saved critical metals can be used for more batteries, electric car or wind turbines in order to accelerate the energy transition. If we add the carbon storage ability of Orange hydrogen, we might just have the solution for some of the energy problems of the coming decades.



521 **Fig. 2** Measured hydrogen in both batch and reactive percolation experiments. In controlled conditions, the production of H₂ is significant and reaches values close to the theoretical maximum. RP = Reactive Percolation

524 7 Corresponding Author

525
526
527 All correspondence should be addressed to F. Osselin (florian.osselin@cnr-
528 orleans.fr).

532 8 Acknowledgment

533
534
535 This research was supported by the LABEX Voltaire (ANR-10-LABX-100-01)
536 and EQUIPEX PLANEX (ANR-11-EQPX-0036).
537
538

541 9 Author contribution

542
543 FO - design of the study, drafting the article and data acquisition. CF - data
544 acquisition. CS, EG and BS revisions. MP - design of the study.
545
546
547
548

549 10 Competing interests

550
551
552 The authors declare no competing interests.

References

- [1] International Energy Agency. World Energy Outlook 2021 - revised version October 2021 (2021). URL www.iaea.org/weo .
- [2] Blanc, P. *et al.* Thermoddem: A geochemical database focused on low temperature water/rock interactions and waste materials. *Applied Geochemistry* **27** (10), 2107–2116 (2012). URL <http://dx.doi.org/10.1016/j.apgeochem.2012.06.002>. <https://doi.org/10.1016/j.apgeochem.2012.06.002> .
- [3] International Energy Agency. The Future of Hydrogen. Tech. Rep., International Energy Agency (2019). URL <https://linkinghub.elsevier.com/retrieve/pii/S1464285912700275>.
- [4] Howarth, R. W. & Jacobson, M. Z. How green is blue hydrogen? *Energy Science and Engineering* **9** (10), 1676–1687 (2021). <https://doi.org/10.1002/ese3.956> .
- [5] Zgonnik, V. The occurrence and geoscience of natural hydrogen: A comprehensive review. *Earth-Science Reviews* **203** (July 2019), 103140 (2020). URL <https://doi.org/10.1016/j.earscirev.2020.103140>. <https://doi.org/10.1016/j.earscirev.2020.103140> .
- [6] Klein, F. *et al.* Iron partitioning and hydrogen generation during serpentinization of abyssal peridotites from 15°N on the Mid-Atlantic Ridge. *Geochimica et Cosmochimica Acta* **73** (22), 6868–6893 (2009). <https://doi.org/10.1016/j.gca.2009.08.021> .
- [7] Kelley, D. S. *et al.* A Serpentinite-Hosted Ecosystem: The Lost City Hydrothermal Field. *Science* **307** (5714), 1428–1434 (2005). URL <http://>

- 599 www.sciencemag.org/cgi/doi/10.1126/science.1102556. [https://doi.org/](https://doi.org/10.1126/science.1102556)
600 [10.1126/science.1102556](https://doi.org/10.1126/science.1102556) .
601
602
- 603 [8] Cannat, M., Fontaine, F. & Escartín, J. in *Serpentinization and*
604 *associated hydrogen and methane fluxes at slow spreading ridges* 241–
605 264 (2010). URL [http://www.agu.org/books/gm/v188/2008GM000760/](http://www.agu.org/books/gm/v188/2008GM000760/2008GM000760.shtml)
606 [2008GM000760.shtml](http://www.agu.org/books/gm/v188/2008GM000760/2008GM000760.shtml).
607
608
- 609 [9] Neal, C. & Stanger, G. Hydrogen generation from mantle source rocks in
610 Oman. *Earth and Planetary Science Letters* **66**, 315–320 (1983). URL
611 <http://linkinghub.elsevier.com/retrieve/pii/0012821X83901449>. [https://](https://doi.org/10.1016/0012-821X(83)90144-9)
612 [doi.org/10.1016/0012-821X\(83\)90144-9](https://doi.org/10.1016/0012-821X(83)90144-9) .
613
614
- 615 [10] Worman, S. L., Pratson, L. F., Karson, J. A. & Klein, E. M. Global rate
616 and distribution of H₂ gas produced by serpentinization within oceanic
617 lithosphere. *Geophysical Research Letters* **43** (12), 6435–6443 (2016).
618 URL <http://doi.wiley.com/10.1002/2016GL069066>. [https://doi.org/10.](https://doi.org/10.1002/2016GL069066)
619 [1002/2016GL069066](https://doi.org/10.1002/2016GL069066) .
620
621
- 622 [11] Geymond, U., Ramanaidou, E., Lévy, D., Ouaya, A. & Moretti, I. Can
623 Weathering of Banded Iron Formations Generate Natural Hydrogen? Evi-
624 dence from Australia, Brazil and South Africa. *Minerals* **12** (2) (2022).
625 <https://doi.org/10.3390/min12020163> .
626
627
- 628 [12] Truche, L. *et al.* Hydrogen generation during hydrothermal alteration of
629 peralkaline granite. *Geochimica et Cosmochimica Acta* (2021). URL [https://](https://doi.org/10.1016/j.gca.2021.05.048)
630 doi.org/10.1016/j.gca.2021.05.048. [https://doi.org/10.1016/j.gca.2021.](https://doi.org/10.1016/j.gca.2021.05.048)
631 [05.048](https://doi.org/10.1016/j.gca.2021.05.048) .
632
633
634
635
636
637
638
639
640
641
642
643
644

- [13] Murray, J. *et al.* Abiotic hydrogen generation from biotite-rich granite: A case study of the Soultz-sous-Forêts geothermal site, France. *Applied Geochemistry* **119** (May 2019) (2020). <https://doi.org/10.1016/j.apgeochem.2020.104631> .
- [14] Etiope, G., Schoell, M. & Hosgörmez, H. Abiotic methane flux from the Chimaera seep and Tekirova ophiolites (Turkey): Understanding gas exhalation from low temperature serpentinization and implications for Mars. *Earth and Planetary Science Letters* **310** (1-2), 96–104 (2011). URL <http://dx.doi.org/10.1016/j.epsl.2011.08.001>. <https://doi.org/10.1016/j.epsl.2011.08.001> .
- [15] Gaucher, E. C. New perspectives in the industrial exploration for native hydrogen. *Elements* **16** (1), 8–9 (2020). <https://doi.org/10.2138/gselements.16.1.8> .
- [16] Lefeuvre, N. *et al.* Native H₂ Exploration in the Western Pyrenean Foothills . *Geochemistry, Geophysics, Geosystems* **22** (8), 1–20 (2021). <https://doi.org/10.1029/2021gc009917> .
- [17] Moretti, I., Brouilly, E., Loiseau, K., Prinzhofer, A. & Deville, E. Hydrogen emanations in intracratonic areas: New guide lines for early exploration basin screening. *Geosciences (Switzerland)* **11** (3) (2021). <https://doi.org/10.3390/geosciences11030145> .
- [18] Guélard, J. *et al.* Natural H₂ in Kansas: Deep or shallow origin? *Geochemistry, Geophysics, Geosystems* **18** (5), 1841–1865 (2017). URL <http://doi.wiley.com/10.1002/2016GC006544>. <https://doi.org/10.1002/2016GC006544> .

- 691 [19] Prinzhofer, A., Tahara Cissé, C. S. & Diallo, A. B. Discovery of a large
692 accumulation of natural hydrogen in Bourakebougou (Mali). *International*
693 *Journal of Hydrogen Energy* **43** (42), 19315–19326 (2018). <https://doi.org/10.1016/j.ijhydene.2018.08.193> .
- 697
698 [20] Kularatne, K. *et al.* Simultaneous ex-situ CO₂ mineral sequestration
699 and hydrogen production from olivine-bearing mine tailings. *Applied*
700 *Geochemistry* **95** (May), 195–205 (2018). URL [https://doi.org/10.1016/](https://doi.org/10.1016/j.apgeochem.2018.05.020)
701 [j.apgeochem.2018.05.020](https://doi.org/10.1016/j.apgeochem.2018.05.020). [https://doi.org/10.1016/](https://doi.org/10.1016/j.apgeochem.2018.05.020)
702 [j.apgeochem.2018.05.](https://doi.org/10.1016/j.apgeochem.2018.05.020)
703 [020](https://doi.org/10.1016/j.apgeochem.2018.05.020) .
- 704
705
706 [21] Kelemen, P. B. *et al.* Rates and Mechanisms of Mineral Carbon-
707 ation in Peridotite: Natural Processes and Recipes for Enhanced, in
708 situ CO₂ Capture and Storage. *Annual Review of Earth and Plane-*
709 *tary Sciences* **39** (1), 545–576 (2011). URL [http://www.annualreviews.](http://www.annualreviews.org/doi/10.1146/annurev-earth-092010-152509)
710 [org/doi/10.1146/annurev-earth-092010-152509](http://www.annualreviews.org/doi/10.1146/annurev-earth-092010-152509). [https://doi.org/10.1146/](https://doi.org/10.1146/annurev-earth-092010-152509)
711 [annurev-earth-092010-152509](https://doi.org/10.1146/annurev-earth-092010-152509) .
- 712
713
714
715
716
717 [22] Kelemen, P. *et al.* In situ carbon mineralization in ultramafic rocks:
718 Natural processes and possible engineered methods. *Energy Procedia*
719 **146** (August), 92–102 (2018). URL [https://linkinghub.elsevier.com/](https://linkinghub.elsevier.com/retrieve/pii/S1876610218301450)
720 [retrieve/pii/S1876610218301450](https://linkinghub.elsevier.com/retrieve/pii/S1876610218301450). [https://doi.org/10.1016/j.egypro.2018.](https://doi.org/10.1016/j.egypro.2018.07.013)
721 [07.013](https://doi.org/10.1016/j.egypro.2018.07.013) .
- 722
723
724
725
726 [23] Gaillardet, J., Dupré, B., Louvat, P. & Allègre, C. J. Global silicate
727 weathering and CO₂ consumption rates deduced from the chemistry of
728 large rivers. *Chemical Geology* **159** (1-4), 3–30 (1999). [https://doi.org/](https://doi.org/10.1016/S0009-2541(99)00031-5)
729 [10.1016/S0009-2541\(99\)00031-5](https://doi.org/10.1016/S0009-2541(99)00031-5) .
- 730
731
732
733
734
735
736

- [24] Matter, J. M. & Kelemen, P. B. Permanent storage of carbon dioxide in geological reservoirs by mineral carbonation. *Nature Geoscience* **2** (12), 837–841 (2009). URL <http://www.nature.com/articles/ngeo683>. <https://doi.org/10.1038/ngeo683> .
- [25] Gíslason, S. R., Sigurdardóttir, H., Aradóttir, E. S. & Oelkers, E. H. A *brief history of CarbFix: Challenges and victories of the project's pilot phase*, Vol. 146 (2018).
- [26] Snæbjörnsdóttir, S. *et al.* Carbon dioxide storage through mineral carbonation. *Nature Reviews Earth and Environment* **1** (2), 90–102 (2020). <https://doi.org/10.1038/s43017-019-0011-8> .
- [27] McGrail, B. P. *et al.* Wallula Basalt Pilot Demonstration Project: Post-injection Results and Conclusions. *Energy Procedia* **114** (November 2016), 5783–5790 (2017). URL <http://dx.doi.org/10.1016/j.egypro.2017.03.1716>. <https://doi.org/10.1016/j.egypro.2017.03.1716> .
- [28] Combaudon, V. & Moretti, I. Generation of Hydrogen along the Mid-Atlantic Ridge: Onshore and Offshore. *Geology, Earth & Marine Sciences* **3** (4), 1–14 (2021). <https://doi.org/10.31038/gems.2021343> .
- [29] Voigt, M. *et al.* An experimental study of basalt–seawater–CO₂ interaction at 130 °C. *Geochimica et Cosmochimica Acta* **308**, 21–41 (2021). <https://doi.org/10.1016/j.gca.2021.05.056> .
- [30] Lawley, C. J. *et al.* Precious metal mobility during serpentinization and breakdown of base metal sulphide. *Lithos* **354–355** (2020). <https://doi.org/10.1016/j.lithos.2019.105278> .

- 783 [31] Lagneau, V., Regnault, O. & Descostes, M. Industrial Deployment of
 784 Reactive Transport Simulation: An Application to Uranium In situ Recov-
 785 ery. *Reviews in Mineralogy and Geochemistry* **85** (1), 499–528 (2019).
 786 <https://doi.org/10.2138/rmg.2019.85.16> .
 787
 788
 789
- 790 [32] Stringfellow, W. T. & Dobson, P. F. Technology for Lithium Extrac-
 791 tion in the Context of Hybrid Geothermal Power. *PROCEEDINGS, 46th*
 792 *Workshop on Geothermal Reservoir Engineering* (2021) .
 793
 794
 795
- 796 [33] O'Connor, W. *et al.* Aqueous Mineral Carbonation: Mineral Availability,
 797 Pretreatment, Reaction Parametrics, and Process Studies. *Doe/Arc-*
 798 *Tr-04-002* (April), 1–19 (2005). URL [https://www.netl.doe.gov/](https://www.netl.doe.gov/FileLibrary/Research/Coal/NETLAlbanyAqueousMineralCarbonation.pdf)
 799 [FileLibrary/Research/Coal/NETLAlbanyAqueousMineralCarbonation.](https://www.netl.doe.gov/FileLibrary/Research/Coal/NETLAlbanyAqueousMineralCarbonation.pdf)
 800 [pdf.](https://www.netl.doe.gov/FileLibrary/Research/Coal/NETLAlbanyAqueousMineralCarbonation.pdf) <https://doi.org/10.13140/RG.2.2.23658.31684> .
 801
 802
 803
 804
- 805 [34] Oelkers, E. H., Declercq, J., Saldi, G. D., Gislason, S. R. & Schott, J.
 806 Olivine dissolution rates: A critical review. *Chemical Geology* **500** (Octo-
 807 ber), 1–19 (2018). <https://doi.org/10.1016/j.chemgeo.2018.10.008> .
 808
 809
 810
- 811 [35] Wang, J., Watanabe, N., Okamoto, A., Nakamura, K. & Komai,
 812 T. Pyroxene control of H₂ production and carbon storage
 813 during water-peridotite-CO₂ hydrothermal reactions. *Inter-*
 814 *national Journal of Hydrogen Energy* **44** (49), 26835–26847
 815 (2019). URL <https://doi.org/10.1016/j.ijhydene.2019.08.161><https://linkinghub.elsevier.com/retrieve/pii/S0360319919331799>. <https://doi.org/10.1016/j.ijhydene.2019.08.161> .
 816
 817
 818
 819
 820
 821
 822
 823
- 824 [36] Chizmeshya, A. V. G., McKelvy, M. J., Squires, K., Carpenter, R. W.
 825 & Bearat, H. A Novel Approach to Mineral Carbonation: Enhancing
 826 Carbonation While Avoiding Mineral Pretreatment Process Cost. *Tech.*
 827
 828

- Rep., Arizon State University (2007). URL <http://www.osti.gov/servlets/purl/924162-e8RuYF/>. arXiv:1011.1669v3. 829
830
831
832
- [37] Lamadrid, H. M., Zajacz, Z., Klein, F. & Bodnar, R. J. Synthetic 833
Fluid Inclusions XXIII . Effect of temperature and fluid composition on 834
rates of serpentinization of olivine. *Geochimica et Cosmochimica Acta* 835
(2020). URL <https://doi.org/10.1016/j.gca.2020.08.009>. [https://doi.org/](https://doi.org/10.1016/j.gca.2020.08.009) 836
[10.1016/j.gca.2020.08.009](https://doi.org/10.1016/j.gca.2020.08.009) . 837
838
839
840
841
- [38] Kelemen, P. B. & Matter, J. M. In situ carbonation of peridotite for 842
CO₂ storage. *Proceedings of the National Academy of Sciences* **105** (45), 844
17295–17300 (2008). <https://doi.org/10.1073/pnas.0805794105> . 845
846
847
- [39] Gunnarsson, I. *et al.* The rapid and cost-effective capture and sub- 848
surface mineral storage of carbon and sulfur at the CarbFix2 site. 849
International Journal of Greenhouse Gas Control **79** (August), 117–126 850
(2018). URL <https://doi.org/10.1016/j.ijggc.2018.08.014>. [https://doi.](https://doi.org/10.1016/j.ijggc.2018.08.014) 851
[org/10.1016/j.ijggc.2018.08.014](https://doi.org/10.1016/j.ijggc.2018.08.014) . 852
853
854
855
856
- [40] Klein, F. *et al.* Fluids in the Crust. Experimental constraints on fluid- 857
rock reactions during incipient serpentinization of harzburgite. *American* 858
Mineralogist **100** (4) (2015). <https://doi.org/10.2138/am-2015-5112> . 859
860
861
862
- [41] Grozeva, N. G., Klein, F., Seewald, J. S. & Sylva, S. P. Experimental study 863
of carbonate formation in oceanic peridotite. *Geochimica et Cosmochim-* 864
ica Acta **199**, 264–286 (2017). URL [http://dx.doi.org/10.1016/j.gca.2016.](http://dx.doi.org/10.1016/j.gca.2016.10.052) 865
[10.052](http://dx.doi.org/10.1016/j.gca.2016.10.052)<https://linkinghub.elsevier.com/retrieve/pii/S001670371630655X>. 866
<https://doi.org/10.1016/j.gca.2016.10.052> . 867
868
869
870
871
872
873
874

- 875 [42] Fauguerolles, C. *Etude Expérimentale de la production d'H₂ associée à la*
876 *serpentinisation des péridotites au niveau des dorsales océaniques lentes.*
877
878 Ph.D. thesis, Université d'Orléans (2016).
879
880
- 881 [43] Osselin, F., Pichavant, M., Champallier, R., Ulrich, M. & Raimbourg,
882 H. Reactive transport experiments of coupled carbonation and serpen-
883 tinization in a natural serpentinite. Implication for hydrogen produc-
884 tion and carbon geological storage. *Geochimica et Cosmochimica Acta*
885 **318**, 165–189 (2022). URL [https://linkinghub.elsevier.com/retrieve/pii/](https://linkinghub.elsevier.com/retrieve/pii/S0016703721006943)
886 [S0016703721006943](https://linkinghub.elsevier.com/retrieve/pii/S0016703721006943). <https://doi.org/10.1016/j.gca.2021.11.039> .
887
888
889
- 890
- 891 [44] Menzel, M. D. *et al.* Carbonation of mantle peridotite by CO₂-rich fluids:
892 the formation of listvenites in the Advocate ophiolite complex (Newfound-
893 land, Canada). *Lithos* **323** (2018). [https://doi.org/10.1016/j.lithos.2018.](https://doi.org/10.1016/j.lithos.2018.06.001)
894 [06.001](https://doi.org/10.1016/j.lithos.2018.06.001) .
895
896
897
898
- 899 [45] Jamtveit, B., Austrheim, H. & Malthes-Sorensen, A. Accelerated hydra-
900 tion of the Earth's deep crust induced by stress perturbations. *Nature*
901 **408** (6808), 75–78 (2000). <https://doi.org/10.1038/35040537> .
902
903
904
- 905 [46] Osselin, F. *et al.* Stress from NaCl crystallisation by carbon dioxide injec-
906 tion in aquifers. *Environmental Geotechnics* **2** (5), 280–291 (2015). URL
907 <http://www.icevirtuallibrary.com/doi/10.1680/envgeo.13.00057>. [https://](https://doi.org/10.1680/envgeo.13.00057)
908 doi.org/10.1680/envgeo.13.00057. [https://](https://doi.org/10.1680/envgeo.13.00057)
909 doi.org/10.1680/envgeo.13.00057 .
910
911
- 912 [47] Zhu, W. *et al.* Experimental evidence of reaction-induced fracturing dur-
913 ing olivine carbonation. *Geophysical Research Letters* **43** (18), 9535–9543
914 (2016). <https://doi.org/10.1002/2016GL070834> .
915
916
917
918
919
920

- [48] van Noort, R., Wolterbeek, T., Drury, M., Kandianis, M. & Spiers, C. 921
 The Force of Crystallization and Fracture Propagation during In-Situ 922
 Carbonation of Peridotite. *Minerals* **7** (10), 190 (2017). URL <http://www.mdpi.com/2075-163X/7/10/190>. <https://doi.org/10.3390/min7100190> . 923
 924
 925
 926
 927
- [49] Luhmann, A. J. *et al.* Chemical and physical changes during seawater 928
 flow through intact dunite cores: An experimental study at 150–200 929
 °C. *Geochimica et Cosmochimica Acta* **214**, 86–114 (2017). URL 930
<http://dx.doi.org/10.1016/j.gca.2017.07.020>. <https://doi.org/10.1016/j.gca.2017.07.020> . 931
 932
 933
 934
 935
 936
- [50] International Energy Agency. The Role of Critical 937
 Minerals in Clean Energy Transitions – Analysis – 938
 IEA. Tech. Rep. (2021). URL <https://www.iea.org/reports/the-role-of-critical-minerals-in-clean-energy-transitions/executive-summary>. 939
 940
 941
 942
 943
 944
 945
 946
 947
 948
 949
 950
 951
 952
 953
 954
 955
 956
 957
 958
 959
 960
 961
 962
 963
 964
 965
 966